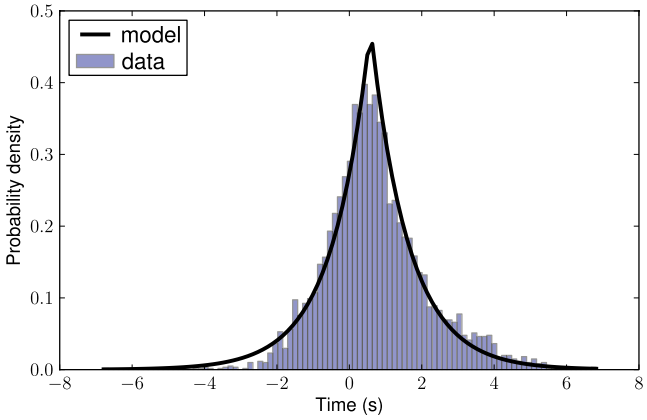

Figure 6. Arrival time distribution around the IASPEI prediction for *P*-phase arrivals at station ASAR. The color version of this figure is available only in the electronic edition.

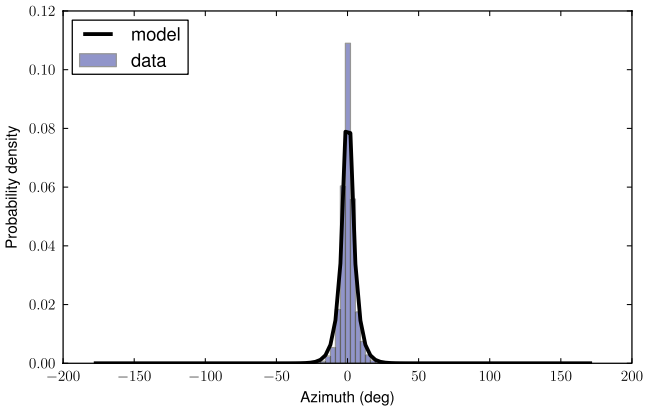

Figure 7. Arrival azimuth distribution around the geographical prediction (plus SASC correction) for *P*-phase arrivals at station ASAR. The color version of this figure is available only in the electronic edition.

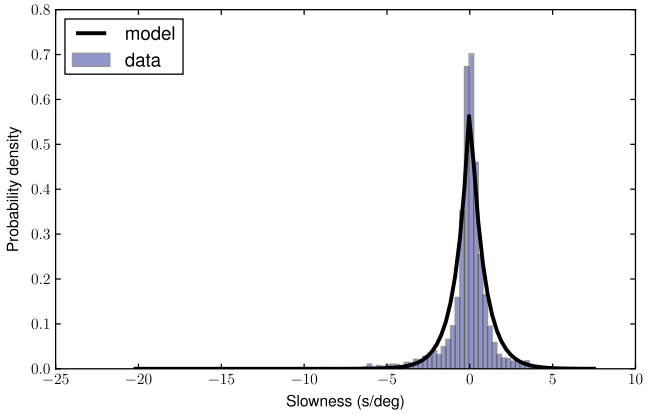

Figure 8. Arrival slowness distribution around the IASPEI prediction (plus SASC correction) for *P*-phase arrivals at station ASAR. The color version of this figure is available only in the electronic edition.

$$P^{jk}_{\phi,z}(\Lambda^{ijk}_z|e^i) = \frac{1}{2b^{jk}_z}\exp\left(-\frac{|\psi[\Lambda^{ijk}_z, G_z(s^k_l, e^i_l)] - \mu^{jk}_z|}{b^{jk}_z}\right),$$

$$P^{jk}_{\phi,s}(\Lambda^{ijk}_s|e^i) = \frac{1}{2b^{jk}_s}\exp\left(-\frac{|\Lambda^{ijk}_s - I^j_s(e^i_d, \Delta_{ik}) - \mu^{jk}_s|}{b^{jk}_s}\right).$$

Here the function ψ computes the difference in the observed angle Λ^{ijk}_z and the angle computed from the geographical function G_z, which depends on the station location, s^k_l, and the event location, e^i_l. Also, I^j_s is the slowness value computed from the IASPEI model for phase j. Technically, the fact that the domain of Laplace distributions is the entire real line makes them inappropriate for azimuth and slowness variables; but the model is reasonable given the small scale of the residuals. It should be noted that the observed values of azimuth and slowness referred to already include certain CTBTO-defined, station-specific corrections called slowness azimuth site corrections (SASC).

The estimation of all the station-and-phase-specific means and scales, for example μ^{jk}_t and b^{jk}_t, is based on a hierarchical model. In this model, each mean and scale is generated from a phase-global prior, which we describe for the arrival time in the following equation:

$$r^{ijk}_t \sim \text{Laplace}(\mu^{jk}_t, b^{jk}_t) \qquad \mu^{jk}_t \sim \text{Laplace}(\mu^j_t, b^j_t)$$
$$(b^{jk}_t)^{-1} \sim \Gamma(1, \beta^j_t) \qquad \mu^j_t \sim \text{Laplace}(0, 100)$$
$$(b^j_t)^{-1} \sim \Gamma(.01, 100) \qquad (\beta^j_t)^{-1} \sim \Gamma(.01, 100).$$

For each phase j, we start by initializing $\mu^{jk}_t = 0$, $b^{jk}_t = 1$ for all stations k, $\mu^j_t = 0$, $b^j_t = 1$, and $\beta^j_t = 1$. Next, we iteratively optimize the values of μ^{jk}_t, b^{jk}_t for each station, and the global values μ^j_t, b^j_t, and β^j_t. This is repeated until convergence. Each of these optimization steps has a simple closed-form solution. A similar procedure is adopted for estimating the azimuth parameters, μ^{jk}_z and b^{jk}_z, and the slowness parameters, μ^{jk}_s, and b^{jk}_s. Examples for these three types of distributions are shown in Figures 6, 7, and 8.

The effect of the hierarchical model is similar in spirit to the model for detection probabilities. For each phase, stations with a lot of data will compute the mean and scale almost exclusively from their own data, whereas parameters for data-poor stations will tend to reflect the global average.

The arrival amplitude Λ^{ijk}_a is similar to the detection probability because it depends only on the event magnitude, depth, and distance to the station. We model the log of the amplitude via a linear regression model with Gaussian noise,

$$r^{ijk}_a = \log(\Lambda^{ijk}_a) - \sum_{w\in\mathcal{F}_a} \mu^{wjk}_a \cdot w[e^i_m, e^i_d, I^j_T(e^i_d, \Delta_{ik})],$$

$$r^{ijk}_a \sim \mathcal{N}(0, \sigma^{jk}_a),$$

where $\mathcal{F}_a$ is a set of feature functions (see Table 3), and μ^{wjk}_a is the weight for feature w. This implies that

$$P^{jk}_{\phi,a}(\Lambda^{ijk}_a|e^i) = \frac{1}{\sqrt{2\pi}\sigma^{jk}_a}\exp\left[-\frac{(r^{ijk}_a)^2}{2\sigma^{jk2}_a}\right]\frac{1}{\Lambda^{ijk}_a}.$$